THERMAL DECOMPOSITION AND CHEMISM OF HYDRONIUM JAROSITE

Miloslav HARTMAN, Václav VESELÝ and Karel JAKUBEC

Institute of Chemical Process Fundamentals,
Czechoslovak Academy of Sciences, 165 02 Prague 6-Suchdol

Received May 8th, 1986

A study is reported of the controlled decompositions and chemism of the technological hydronium jarosite. Chemical and spectroscopic methods were employed to determine the amounts of impurities present in jarosite. Thermogravimetric data were amassed both in the increasing and constant temperature mode. Proposed kinetic equations of Arrhenius type were tested against the results of constant temperature experiments. Differences are explored in the course of the decomposition of hydronium jarosite and that of pure ferric sulphate enneahydrate. In addition, the effects of temperature and reaction time were investigated on the amount of sulphates remaining in the calcined particles.

The jarosites are compounds of the type $MFe_3^{3+}(SO_4)_2(OH)_6$, where M is H_3O^+, Na^+, K^+, Rb^+, Ag^+, Tl^+, NH_4^+, $1/2\,Pb^{2+}$ or $1/2\,Hg^{2+}$ and where some substitutions can occur for Fe^{3+} and SO_4^{2-} (ref.[1]). Their precipitates can easily be settled, filtered and washed. Thus, they provide possible means for the elimination of iron, sulphate, alkalis and other components from hydrometallurgical solutions[2]. Recent experience shows, however, that some other metals are significantly co-precipitated with jarosites.

Most of the recent research has been directed to sodium, ammonium and potassium jarosite. Little work has been done with hydronium jarosite. Hydronium jarosite is precipitated from the iron-rich, acid solution at elevated temperature and pressure. The precipitate is a readily filterable product which is discarded or further treated. It appears that it may be utilized to produce Fe_2O_3 for either the metal or pigment industries by the calcination of jarosite residues.

The results previously reported[3] showed that hydronium jarosite decomposes in two stages. Water is released rapidly at 450°C according to the reaction

$$H_3OFe_3(SO_4)_2(OH)_6\,(s) = \tfrac{2}{3}Fe_2(SO_4)_3\,(s) + \tfrac{5}{6}Fe_2O_3\,(s) + \tfrac{9}{2}H_2O\,(g)\,. \qquad (A)$$

Sulphur oxides are readily released at 650–700°C

$$Fe_2(SO_4)_3\,(s) = Fe_2O_3\,(s) + 3\,SO_3\,(g)\,. \qquad (B)$$

The overall thermal decomposition can be represented as follows:

$$H_3OFe_3(SO_4)_2(OH)_6\,(s) = \tfrac{3}{2}Fe_2O_3\,(s) + \tfrac{9}{2}H_2O\,(g) + 2\,SO_3\,(g)\,. \qquad (C)$$

The reaction (*C*) is strongly endothermic with $\Delta H_r^{25°C} = 1\,098{\cdot}3$ kJ mol^{-1} (ref.[3]). The purpose of this paper is to describe the kinetics of the decomposition reactions, explore the chemism of the technological hydronium jarosite and examine the effects of operating conditions on the rate of decomposition.

RESULTS AND DISCUSSION

Chemical Composition of Hydronium Jarosite

Whole work has been carried out with the technological hydronium jarosite produced in a pilot plant. This hydrometallurgical pilot plant processes the sulphide, collective concentrates containing 18—22% Zn, 8—10% Pb, 2—3% Cu, 23—28% Fe and 32—37% S by weight. With respect to its origin the sample was analyzed for sulphur, iron, zinc, aluminum, silicon, sodium, potassium, phosphorus, calcium, magnesium, arsenic, antimony, copper, cadmium, and lead. Results of the chemical analyses are presented in Table I. The analysis suggests that there is a slight deficiency of sulphates relative to iron.

The fractions of zinc, aluminium and silica amount to more than 1% by weight. The sample contains more than 0·5% by weight of sodium, potassium and phosphates. The fractions of calcium, magnesium and arsenic are higher than 0·2% by weight.

Semi-quantitative spectroscopic analyses were made of the jarosite particles calcined at 800°C. Results of these analyses are summarized in Table II. The results of both analyses are in general agreement. They show that the main impurities of hydronium jarosite are zinc, aluminum, silicon, sodium, potassium, phosphorus, calcium and magnesium. It is of interest to note the presence of a smaller amount of indium revealed by spectroscopy. It appears that zinc, aluminum and silicon can co-precipitate to some extent with hydronium jarosite. The above findings also support the idea of mutual interchangeability of the hydronium, sodium and potassium ions. As can be seen

TABLE I

Chemical analysis of technological hydronium jarosite

Component	wt. %	Component	wt. %
SO_4^{2-}	33·69	Ca	0·301
Fe	33·14	MgO	0·25
Zn	1·50	As_2O_5	0·22
Al	1·14	Sb	0·10
SiO_2	1·04	Cu	0·057
Na	0·885	Cd	0·02
PO_4^{3-}	0·711	Pb	$5 \cdot 10^{-4}$
K	0·573	H_2O at 105°C	4·2

in Table I and Table II, there may be some uncertainty in the amount of lead found by the respective analytical methods.

TGA *Experiments*

Decomposition experiments were performed with the powdered samples at a constant rate of temperature increase and with small pellets at constant temperature. The apparatus used for temperature increase runs was a commercial instrument (Stanton Redcroft). In order to conform to common practice, all experiments were carried out on 50 mg samples. Particle size ranged from 30 to 90 μm. A nitrogen flow of 100 cm^3 min^{-1} was maintained through the apparatus to remove the gaseous products of reaction. After preliminary tests TGA runs were conducted at a heating rate of 7 °C min^{-1}. In the course of the experiments, the weight was recorded as a function of temperature and time.

The decomposition experiments at constant temperature were conducted in a differential reactor. Air passed through a thin, fixed layer of pellets at a superficial velocity of 1 m s^{-1}. Further details on the reactor design can be found elsewhere[4]. The degree of decomposition of pellets (about 50 mg hydronium jarosite) was determined as weight loss.

The paste of jarosite sample was extruded through a coarse sieve. The formed extrudate was dried at 60°C, crushed and sieved. A fraction of the pellets selected within the range 0·50—0·63 mm ($\bar{d}_p$ = 0·565 mm) was employed in this work.

Two large waves were detected on the TGA curve of hydronium jarosite. The first was in the range 325—415°C corresponding to the release of water. The second wave corresponding to the release of SO_2 and SO_3 was located in the range 570—720°C. The curves are presented in Figs 1 and 2. The wide plateau in the temperature interval 415 to 570°C shows that the two decomposition steps are completely independent. Small, but appreciable weight loss was recorded in the range 850—1 050°C. This finding indicates the presence of thermally more stable compounds in hydronium jarosite.

Reaction Kinetics

A knowledge of kinetic behaviour is essential for predicting the thermal behaviour of jarosite decomposition processes. Thermogravimetric analysis provides a semi-

TABLE II

Semi-quantitative spectroscopic analysis of calcined particles of hydronium jarosite

Element	wt. %
Fe, Zn, Si, Pb	> 1
Al, K, Na, As, Ca, In	0·1—1
Cu, Mn, Sb, Sn	0·01—0·1
Ag, Cr, Mo, Ba, Bi, Cd, Mg, Sr, Ti, Tl, V, W	0·001—0·01

quantitative description of the decomposition reactions under well-controlled laboratory condition. By the use of small sample mass and fine powders, heat and mass transfer effects can be greatly reduced. The increasing temperature data plotted in Figs 1 and 2 can serve as a suitable base for development of kinetic equations describing the course of the calcination of jarosite particles.

It is not anticipated that a single kinetic equation would describe the decompositions of this study. The decomposition rate of a solid can be represented by the general rate expression

$$\frac{dX}{d\tau} = k_0(1 - X)^n \exp(-E/RT) . \qquad (1)$$

This equation accounts for possible effects of nucleation and diffusion on the rate of decomposition. It reduces to the Jerofeev equation for $n = 1$; it conforms to the three-dimensional and two-dimensional shrinking core models for $n = 1/3$ and $n = 1/2$, respectively. The equation follows the Avrami nucleation law (constant density of nuclei and one-dimensional nucleus growth) with $n = 0$ (refs[5,6]).

The experimental data from the both decomposition runs were tested empirically by fitting to the linearized form of Eq. (1)

$$\ln\left(\frac{dX/d\tau}{(1 - X)^n}\right) = -\frac{E}{R} \cdot \frac{1}{T} + \ln k_0 . \qquad (2)$$

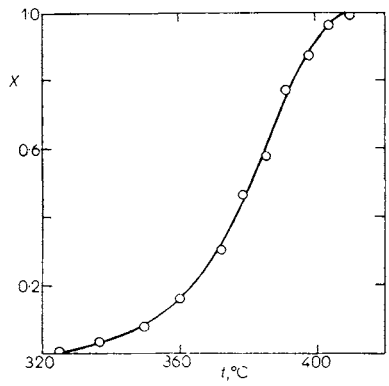

FIG. 1

Experimental results for the first stage of decomposition of hydronium jarosite; increasing temperature run, original sample mass 50 mg, heating rate 7°C min^{-1}

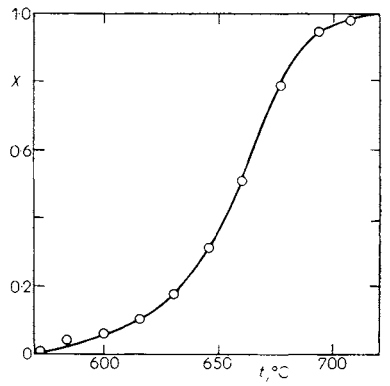

FIG. 2

Experimental results for the second stage of decomposition of hydronium jarosite; increasing temperature run, original sample mass 50 mg, heating rate 7°C min^{-1}

Values of the reaction rate, $dX/d\tau$, were determined from the curve X *vs* τ at equal conversion intervals. At least twenty points were taken in each series to fit Eq. (*2*). When the order of reaction, n, was found by a trial and error procedure, the other kinetic parameters were computed by a least-squares method. The activation energy, E, and frequency factor, k_0, determined from the slope and ordinate intercept of the best-fit straight line are summarized in Table III. The dehydration data points lie on a straight line for $n = 0{\cdot}8$. The data points for the release of sulphur oxides behave linearly for $n = 1$. As can be seen in Figs 3 and 4, the data points reasonably fit straight lines for the respective values of n.

In order to explore accuracy of the kinetic parameters, Eq. (*2*) was rewritten and the integral

$$\tau = \frac{\exp(E/RT)}{k_0} \int_0^X \frac{dX}{(1 - X)^n} \qquad (3)$$

was evaluated numerically by the trapezoidal rule. In the case of $n = 1$, Eq. (*3*) can easily be solved analytically and takes the form

$$\tau = (-1/A) \cdot \ln(1 - X) \qquad (4a)$$

or

$$X = [\exp(A\tau) - 1]/\exp(A\tau), \qquad (4b)$$

where $A = k_0 \exp(-E/RT)$.

Eqs (*3*) and (*4*) are highly nonlinear and, therefore, considerably sensitive, in general to the variations in values of the kinetic parameters. The conversions computed for different reaction times and temperatures are compared with the corresponding experimental values in Figs 5 and 6. The data points plotted in these figures were

TABLE III

Kinetic parameters of the decomposition reactions of hydronium jarosite

Reaction	Temperature range, °C	Order of reaction, n	Activation energy, E kJ mol^{-1}	Frequency factor, k_0 s^{-1}
Release of water, reaction (*A*)	325—410	0·8	190·6	$7{\cdot}299 \cdot 10^{12}$
Release of SO_2 and SO_3, reaction (*B*)	570—720	1·0	298·0	$1{\cdot}695 \cdot 10^{14}$

obtained from the experiments performed in the isothermal mode. One can see that there are some differences between the predicted and experimental curves. It appears

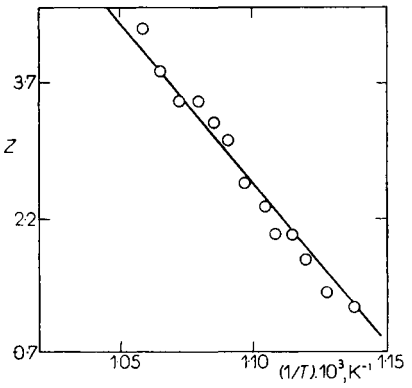

FIG. 3

Correlation of the kinetic data for the first stage of decomposition of hydronium jarosite. The solid line represents the least-squares fit of data

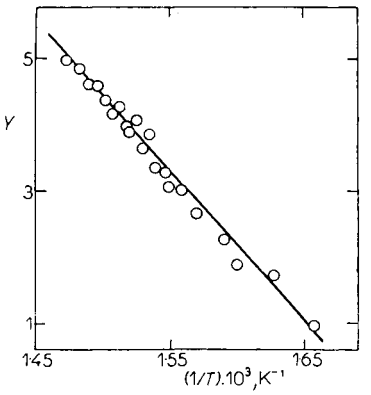

FIG. 4

Correlation of the kinetic data for the second stage of decomposition of hydronium jarosite. The solid line represents the least-squares fit of data

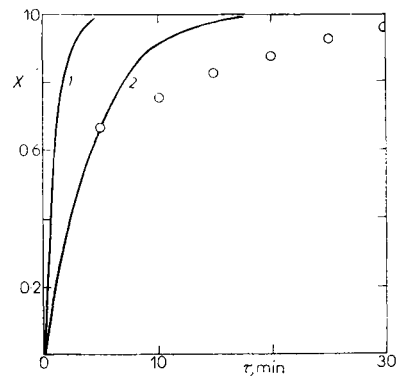

FIG. 5

Thermal decomposition of hydronium jarosite at 400°C (release of water); particle size $\bar{d}_p = 0{\cdot}565$ mm. Predictions of Eq. (*3*) for 400°C (curve *1*), predictions of Eq. (*3*) for 375°C (curve *2*)

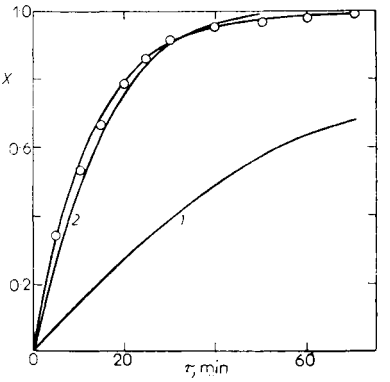

FIG. 6

Thermal decomposition of hydronium jarosite at 600°C (release of SO_2 and SO_3); particle size $\bar{d}_p = 0{\cdot}565$ mm. Predictions of Eq. (*4*) for 600°C (curve *1*), predictions for 630°C (curve *2*); o experimental values from the reactor measurements

as if the computed dependences were somewhat shifted in temperature. It is of interest to note that such shifts in Figs 5 and 6 amount to 20–30°C and occur in the opposite directions.

The different modes of measurements seem to be among the major factors affecting the comparison. It is a common experience that the results of increasing temperature runs are notoriously sensitive to heating rates. Heat transfer can affect the data amassed by constant temperature runs, particularly when the rapid rate of decomposition is combined with the high heat of reaction. Considerable sensitivity of the rate of reaction to temperature should also be considered. In light of these facts the found differences seem to be understandable. We believe that the proposed kinetic equations can be applied to modelling and simulation of a reactor for the thermal decomposition of hydronium jarosite. The empirical correlations developed here have the usual limitations and they should be applied with caution outside the experimental conditions from which they were educed.

Comparison of Thermal Stability of Hydronium Jarosite and Ferric Sulphate Enneahydrate

The sample of $Fe_2(SO_4)_3.9\,H_2O$ used in this work was obtained as Analyzed Reagent Grade. The manufacturer's specification showed putity above 99%.

A fraction of particles 0·8–1·0 mm was separated from the commercial product by sieving. Samples as large as 50 mg were exposed to a moderate flow of air for 10 minutes at temperatures ranging from 200 to 850°C. Results of these experiments are presented in Fig. 7.

As can be seen from the curve in Fig. 7, ferric sulphate releases all crystal water already at 250°C. In contrast to the crystal water in ferric sulphate, the hydronium ions and hydroxyl groups in the molecule of jarosite decompose completely only at 450°C.

Dehydrated ferric sulphate is fully decomposed at 650°C. The weight loss determined at this temperature as large as 0·722 is in good agreement with a stoichiometric value of 0·716. Majority of sulphates present in the dehydrated particles of jarosite

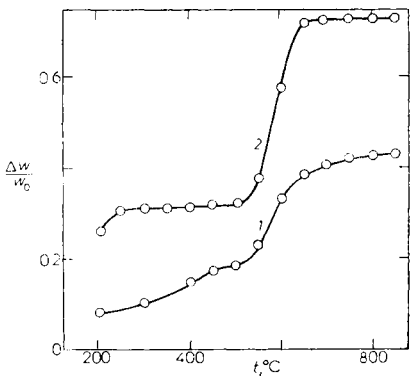

FIG. 7

Dependence of the weight loss of hydronium jarosite (curve 1) and ferric sulphate enneahydrate (curve 2) on the temperature of decomposition; particle size $\bar{d}_p = 0{\cdot}565$ mm, reaction time 10 minutes; o experimental values from the reactor measurements

decompose at 650°C. It is apparent from the Fig. 7 that, in contrast to ferric sulphate, the jarosite curve indicates a moderate, but appreciable increase of weight loss with temperature until a maximum temperature of 850°C is reached.

In order to explore a possible effect of the origin of dehydrated ferric sulphate on its stability, particles of $Fe_2(SO_4)_3.9\,H_2O$ and $H_3OFe_3(SO_4)_2(OH)_6$ were at first dehydrated at 430°C. These dehydrated particles were then used to determine the decomposition rates of sulphates at 600°C. The experimental results are shown in Fig. 8. One should realize that $Fe_2(SO_4)_3$ is the sole, solid product of dehydration of $Fe_2(SO_4)_3.9\,H_2O$. As reaction (*A*) suggests, however, Fe_2O_3 is also formed as water is released from $H_3OFe_3(SO_4)_2(OH)_6$. Therefore, the weight losses measured with $Fe_2(SO_4)_3$ have been related to the same numerical basis according to Eq. (*5*)

$$\left(\frac{\Delta w}{w_0}\right)_{\text{jarosite}} = \frac{Fe_2(SO_4)_3}{Fe_2(SO_4)_3 + \frac{5}{4}Fe_2O_3} \cdot \left(\frac{\Delta w}{w_0}\right)_{Fe_2(SO_4)_3} = 0{\cdot}6670 \left(\frac{\Delta w}{w_0}\right)_{Fe_2(SO_4)_3} \qquad (5)$$

prior to plotting in Fig. 8.

One can see from the curves in Fig. 8 that the two differently formed sulphates decompose at the same rate during first fifteen minutes of exposure. The experimental curves diverge widely at longer times of reaction. The curves differ mainly by the attained weight loss. It follows from stoichiometry that the weight loss of $Fe_2(SO_4)_3$ amounts to 0·601. After correcting on the basis comparable with jarosite, this quantity leads to a value of 0·400. It is apparent from Fig. 8 that the particles of $Fe_2(SO_4)_3$ were entirely decomposed after 50 minutes of exposure at 600°C. The decomposition of jarosite particles proceeds very slowly after this reaction time elapsed. The amount of sulphates in the dehydrated particles suggests an attainable value of weight loss of 0·33. Weight loss actually reached at 600°C amounts only to 0·26. These results indicate that about 20% of sulphates, originally present in jarosite, are combined with cations other than Fe^{3+}.

A comparison of colours of both calcined particles can be of interest. The decomposed particles of jarosite are red-brown with a tint of violet. The calcined particles of pure $Fe_2(SO_4)_2.9\,H_2O$ are somewhat lighter and without the violet tint.

Effect of Temperature and Reaction Time on the Degree of Decomposition of Sulphates

In order to delineate the bounds to which the amount of sulphates can be lowered, two series of experimental measurements were made at 700 and 800°C. At such temperatures the decomposition of ferric sulphate is very rapid, if not instantaneous. In another words, the aim of these experiments was to explore the thermal stability of the other sulphates present in hydronium jarosite. In the experiments, the particles of the original jarosite 0·8 – 1·0 mm were calcined for 10 to 60 minutes. The amounts

of sulphates in the calcined particles were determined by chemical analysis. The results are presented in Fig. 9. As the curves in this figure indicate, the influence of temperature weakens with the increasing time of reaction. The particles calcined for 60 minutes at 700 and 800°C contained 7 and 6·8% SO_4^{2-} by weight, respectively. Combined with the found values of weight loss, these results lead to the overall degree of sulphate conversion as large as 87·7 and 88·2%, respectively.

If we assume that all calcium, sodium and potassium are present in jarosite as sulphates[7], they represent about 10% of the total sulphates. Another 2% of sulphates can be present in the forme of magnesium sulphate. It is likely that the undecomposed fraction of sulphates consists of the stable sulphates of Na, K, Ca and, possibly, Mg. With respect to the complex chemism of samples, their diffraction analysis would be difficult.

CONCLUSIONS

A sample of technological hydronium jarosite contains an appreciable amounts of impurities such as zinc, aluminum, silica, sodium, potassium, phosphates, calcium and magnesium.

Two decomposition steps, the release of water in the first stage and release of sulphur oxides in the second, are completely independent. The reaction kinetics of the both steps can be described, with reasonable accuracy, by two different kinetic expressions educed from the thermogravimetric data. While ferric sulphate enneahydra-

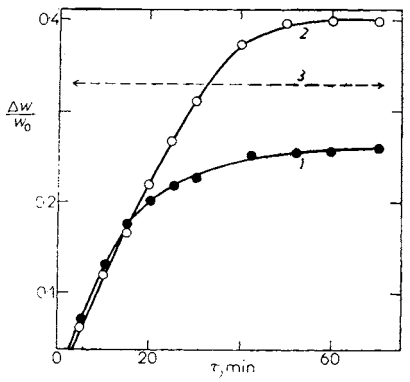

FIG. 8

Comparison of the thermal decomposition of dehydrated ferric sulphate (curve 2) and dehydrated jarosite (curve 1); particle size $\bar{d}_p$ = 0·9 mm, temperature 600°C; complete decomposition of SO_4^{2-} in jarosite (line 3)

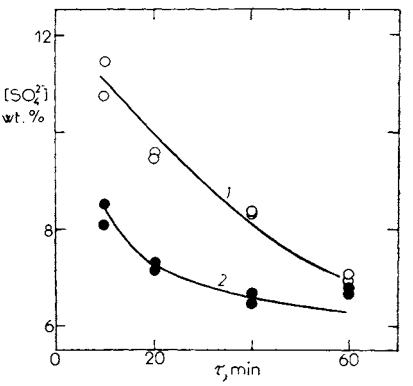

FIG. 9

Influence of temperature and reaction time on the sulphate concentration in the calcined particles. Temperature 700°C (curve 1), temperature 800°C (curve 2)

te, rapidly loses all water at 200–250°C, the dehydration of hydronium jarosite readily takes place at 400–450°C.

Due to the complex chemism of technological hydronium jarosite, the decomposition of the present sulphates is not complete at temperatures below 850°C. Pure ferric sulphate is completely decomposed after an hour of calcination at 600°C. Approximately 90% sulphates contained in jarosite decompose when heated for the same period of time at 800°C. The cause of this fact is probably the presence of sodium, potassium, calcium and magnesium sulphates.

The rate of sulphate decomposition is very sensitive to temperature at temperatures below 700°C. The attainable degree of decomposition slightly increases with the increasing temperature.

LIST OF SYMBOLS

E activation energy (J mol^{-1})
k_0 frequency factor (s^{-1})
ln natural (Naperian) logarithm
n order of reaction
R universal gas constant (8·314 J K^{-1} mol^{-1})
t temperature (°C)
T absolute temperature (K)
w_0 original weight of sample (g)
Δw weight loss due to thermal decomposition (g)
$\Delta w/w_0$ fractional weight loss
X fractional conversion of the decomposing solid
$Y = \ln\left(\frac{(\mathrm{d}X/d\tau) \cdot 10^4}{(1-X)^{0.8}}\right)$ quantity plotted in Fig. 3
$Z = \ln\left(\frac{(\mathrm{d}X/\mathrm{d}\tau) \cdot 10^4}{1-X}\right)$ quantity plotted in Fig. 4
τ time of reaction (s)

REFERENCES

1. Dutrizac J. E., Kaiman S.: Can. Mineral *14*, 151 (1976).
2. Kunda W., Weltman H.: Metall. Trans. *10B*, 439 (1979).
3. Hartman M., Svoboda K., Veselý V., Pata J.: Chem. Prum. *35/60*, 412 (1985).
4. Hartman M.: This Journal *39*, 2374 (1974).
5. Young D. A.: *Decomposition of Solids*, p. 182. Pergamon Press, Oxford 1966.
6. Mu J., Perlmutter D. D.: Ind. Eng. Chem., Process Des. Develop. *20*, 640 (1981).
7. Dutrizac J. E. in the book: *Hydrometallurgy Research. Develapment and Plant Practice* (K. Osseo-Asare and J. D. Miller, Eds), p. 331. Proceedings of the 3rd Int. Symp. on Hydrometallurgy, 112th AIME Ann. Meeting, Atlanta, Georgia, March 6–10, 1983. Published by the Metall. Soc. of AIME, 1982.

Translated by the author (M. H.).